Electronic Supplementary Material (ESI) for Soft Matter.

Supplementary Information

for

Structure-Properties Relationships in Renewable Composites of Poly(lactic acid) Reinforced by Low Amounts of Micro- and Nano- Kraft-Lignin

Sofia P. Makri,[a,b] Panagiotis A. Klonos,[a,c,*] Giacomo Marra,[d] Alexandros Zoikis Karathanasis,[b] Ioanna Deligkiozi,[b] Miguel Ángel Valera,[d] Ana Mangas,[d] Nikolaos Nikolaidis,[a] Zoi Terzopoulou,[a] Apostolos Kyritsis,[c] and Dimitrios N. Bikiaris[a,*]

[a] *Laboratory of Polymer Chemistry and Technology, Department of Chemistry, Aristotle University of Thessaloniki, GR-541 24, Thessaloniki, Greece*

[b] *Creative Nano PC, 43 Tatoiou, Metamorfosi, 14451 Athens, Greece*

[c] *Dielectrics Group, Department of Physics, National Technical University of Athens, Zografou Campus, 15780, Athens, Greece*

[d] *AIMPLAS, Asociación de Investigación de Materiales Plásticos Y Conexas, Carrer de Gustave Eiffel, 4, 46980 Valencia, Spain, Mechanochemistry & Reactive Extrusion*

[*] *Corresponding author: pklonos@central.ntua.gr (P.A.K.); dbic@chem.auth.gr (D.N.B.)*

S1. Additional experimental method

The light flash analysis (LFA) method was employed to evaluate the thermal diffusivity, α, based on the Parker's method[1]. The measurements were conducted by means of a NETZSCH LFA 467 HyperFlash apparatus (NETZSCH, Germany), at RT~22 ^{o}C, on samples in the amorphous state (melt-quenched) and upon subjection to melting and cooling at ~10 K/min. The latter step provided both amorphous and semicrystalline samples (details being given at a later section).

S2. Experimental findings the electrical conductivity and thermal diffusivity

From the same BDS findings, we were able to calculate the electrical AC conductivity, σ_{AC}.[2,3] In Figure S1a, we show the $\sigma_{AC}(f)$ for all samples at two distinct temperatures, namely at 80 ^{o}C (main figure) and at 20 ^{o}C (inset). In general, there systems exhibit low conductivity values. At $T<T_g$ in the inset to Figure S1a, σ_{AC} exhibits a gradually increasing trend with f. None of the materials shows any plateau, which indicates that all systems are practically electrical insulating. At the rubbery state, however ($T>T_g$ e.g., 80 ^{o}C), for the lower frequencies, σ_{AC} is increased up to two orders of magnitude. This phenomenon is due to the involvement of electrical charges orientationally moving throughout the rubbery polymer matrix. In Figure S1b, we present the values of σ_{AC} at the lower frequency of recording. These σ_{AC} vary between 10^{-14} and 10^{-9} S/cm, being such low that denote ionic rather than electronic conductivity. This is expected, as our systems do not occupy free electrons. The phenomena here are compatible with PLA-lignin-based PNCs previously studied by other groups[4].

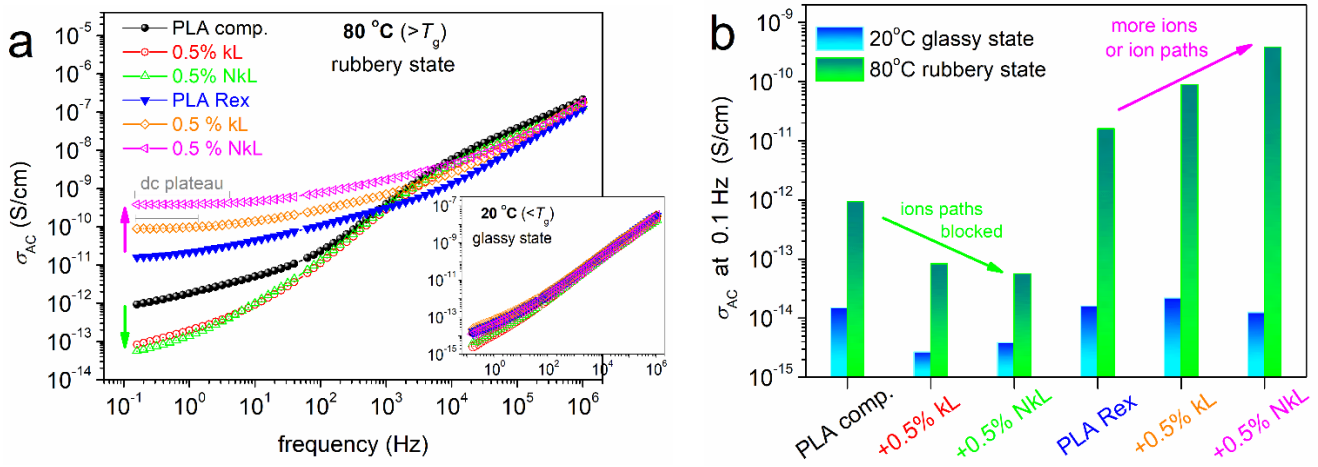

Figure S1. (a) AC electrical conductivity, $\sigma_{AC}(f)$ at 80 ºC (rubbery state) and at 20 ºC (inset, glassy state). (b) Shows the values of σ_{AC}(0.1 Hz) for all samples in the form of column diagrams.

Coming to the effects of lignin at the rubbery state of the polymer, in the PLA-comp series the presence of kL and NkL impose a significant suppression. Most probably, the lignin or/and the lignin-bound polymer entities introduce a kind of blockage to the ions transport via the matrix. On the other hand, the PLA-Rex systems show the higher σ_{AC} values, which is interestingly compatible with the easier chains diffusion (lower T_gs) and possibly more free volume that facilitate the ions transport as well. Here, with the addition of kL and NkL σ_{AC} increases further. Comparing to kL, NkL imposes the stronger effect; furthermore, a narrow plateau is even recorded for this PNC. This is the so called 'DC plateau' wherein σ_{AC} becomes independent from f. We believe that this is also connected with the further mobilization of the polymer chains in the PNCs. Thus, we indirectly conclude that the PLA-Rex systems filled with NkL provide the best charge transport properties. Contrariwise, the PLA-comp filled with kL and NkL demonstrate the poorest ionic conductivity.

Last but not least, we present the data on heat transport studied by the LFA method[1,5]. In Figure S2, we present directly the thermal diffusivity, α, at RT for all samples. The results are shown for polymers in the amorphous state, kept by melting and fast cooling, and upon melt and slow cooling. The latter process, according to calorimetry, resulted in amorphous PLA-comp and semicrystalline PLA-Rex.

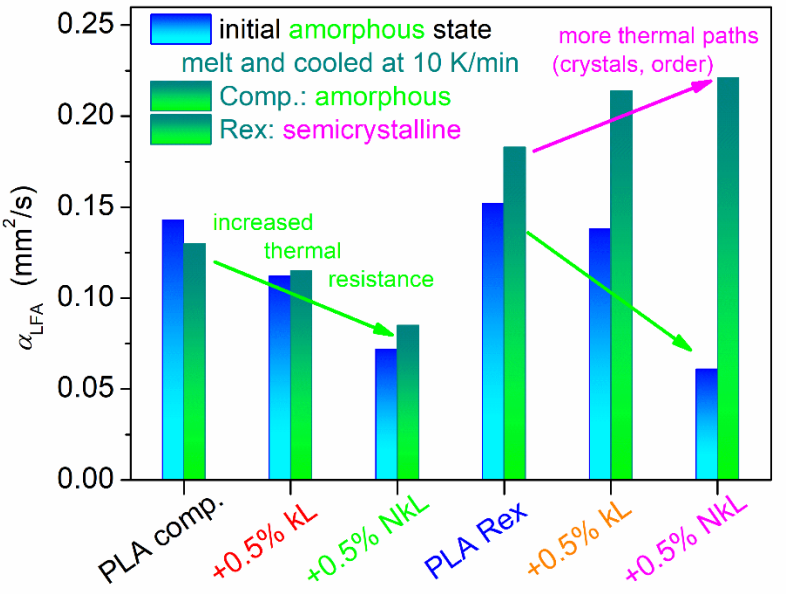

Figure S2. The thermal diffusivity, α_{LFA}, at T~RT for all samples at the amorphous and semicrystalline state. The added arrows mark the effects of the kL and NkL addition in PLA.

Unfortunately, to the best of our knowledge, there are no previous works on the effects of lignin on the thermal diffusivity/conductivity of PLA to compare with. Thus, our structure-properties relationships here will be inevitably based on the present observations along with previous knowledge on different systems. Since the situation and the physical processes are complex, to help the discussion, we created the schemes of Figure S3, which are based on previous knowledge and are fitted to the present findings.

In general, our systems exhibit low α values, i.e., 0.06-0.22 mm^2/s (Figure S2), which is expected for polymers[5-7]. In the amorphous state, kL and NkL seem to lead to a decrease in α of ~15-30%. We recall the quite low amount of lignin loading, thus, the α decrease does not only originate on the non-thermally conducting character of lignin, but, on the introduction of significant interfacial or contact thermal resistance effects[6,8] (schemes in Figure S3a). The effect is stronger by NkL than by kL, which

provides an additional indirect indication of the stronger impact of the 'nano-' lignin as well as of the good lignin dispersion.

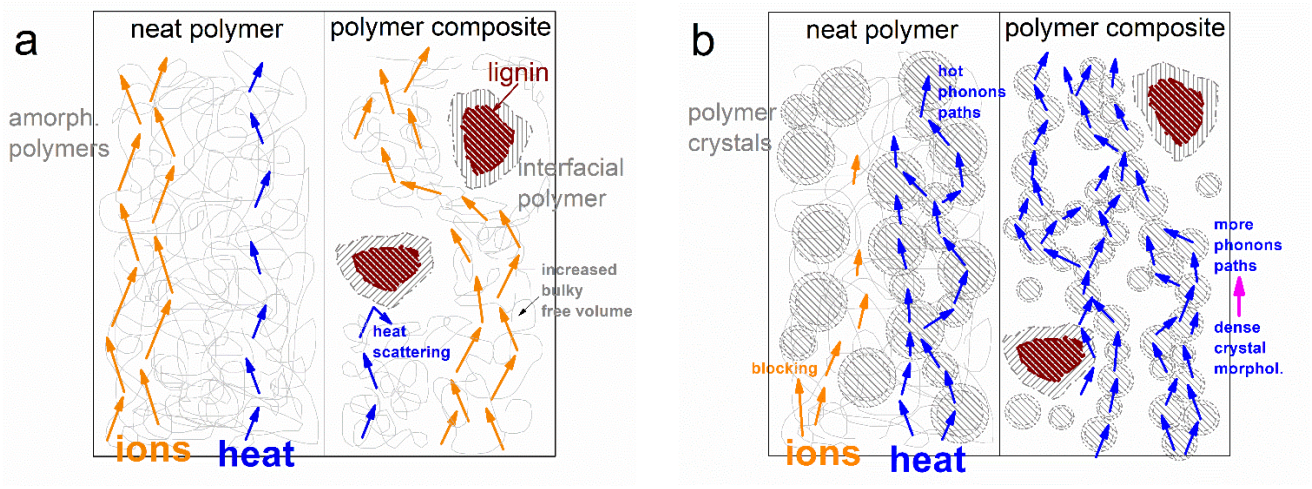

Figure S3. Simplified model schemes to describe the realistic scenario on the physical processes on heat and ions transport[3,5-7] via a neat polymer, PLA here, and a corresponding composite, PLA/lignin here, in the (a) amorphous and (b) semicrystalline state. The model is fitted on the present case, e.g., the recorded sparce or denser semicrystalline morphology in the polymer and the PNC, respectively, as well as the estimated changes in the free volume of the bulky polymer.

The implementation of crystallinity in PLA-Rex introduces opposite and quite more interesting effects. It is known that, compared to amorphous polymers, the semicrystalline ones demonstrate an improved transfer of heat[7,9]. This is due to the crystals-induced order (polymer chains folded and packed/oriented within the crystals), subsequently, increasing of 'phonons' which are the most efficient carriers for heat (thermal energy) transfer (please compare Figures S3a and b). We have recently proposed that next to the existence of crystals, the formation of continuous crystal paths, i.e., the degree of crystals-interconnectivity, facilitates further the transport of heat throughout a polymer matrix (Figure S3b)[3,5]. This happens here in the case of the PLA-Rex systems, including the unfilled matrix, as a systematic increase in α is observed when changing from the amorphous to the semicrystalline state. In particular, there is recorded an α increase, $\Delta\alpha$, of ~13% in neat PLA-Rex, ~50% in PLA-Rex+0.5% kL

and, strikingly, ~200% in PLA-Rex+0.5% NkL. Comparing to the crystalline fraction values (Table 1 in the main article), the CF changes do not directly fit with the $\Delta\alpha$. Whereas, $\Delta\alpha$ seems to fit better with the concept of the crystals-interconnectivity and this is better supported by the corresponding 'loose to denser semicrystalline morphology' changes recorded by PLM (Figure 6 in the main article), especially for PLA-Rex+0.5% NkL.

References

1. W.J. Parker, R.J. Jenkins, C.P. Butler and G.L. Abbott, *J. Appl. Phys*., 1961, **32**, 1679.
2. E. Logakis, E. Pollatos, Ch. Pandis, V. Peoglos, I. Zuburtikudis, C.G. Delidis, A. Vatalis, M. Gjoka, E. Syskakis, K. Viras and P. Pissis, *Compos. Sci. Technol.*, 2010, **70**, 328–335.
3. P.A. Klonos, L. Papadopoulos, D. Kourtidou, K. Chrissafis, V. Peoglos, A. Kyritsis and D.N. Bikiaris, *Applied Nano*, 2022, **2**, 31–45.
4. J. Fal, K. Bulanda, J. Traciak, J. Sobczak, R. Kuzioła, K.M. Grąz, G. Budzik, M. Olesky and G. Żyła, *Molecules*, 2020, **25**, 1354.
5. P.A. Klonos, V. Peoglos, D.N. Bikiaris and A. Kyritsis, *J. Phys. Chem. C*, 2020, **123**, 5469–5479.
6. Z. Han and A. Fina, *Prog. Polym. Sci.*, 2011, **36**, 914–944.
7. D. Hansen and G.A. Bernier, *Polym. Eng. Sci.*, 1972, **12**, 204–208.
8. P. Ding, S. Su, N. Song, S. Tang, Y. Liu and L. Shi, *RSC Advances*, 2014, **4**, 18782–18791.
9. J.J. Marsh, R.P. Turner, J. Carter and M.J. Jenkins, *Polymer*, 2019, **179**, 121595.